Hybrid Simulation-Measurement Method for Broadband Dielectric Characterization of Synthetic Human Head Tissues

Hybrid Simulation-Measurement Method for Broadband Dielectric Characterization of Synthetic Human Head Tissues

Martina Gugliermino
Dept. of Electronics and Telecommunications Politecnico di Torino
Torino, Italy
martina.gugliermino@polito.it

David O. Rodriguez-Duarte
Dept. of Electronics and Telecommunications Politecnico di Torino
Torino, Italy
david.rodriguez@polito.it

Jorge A. Tobon Vasquez
Dept. of Electronics and Telecommunications Politecnico di Torino
Torino, Italy
jorge.tobon@polito.it

Mauro Lumia
National Research Council, Inst. of Electronics and Information and Telecommunications Engineering
Torino, Italy
mauro.lumia@ieiit.cnr.it

Giuseppe Virone
National Research Council, Inst. of Electronics and Information and Telecommunications Engineering
Torino, Italy
giuseppe.virone@ieiit.cnr.it

Francesca Vipiana
Dept. of Electronics and Telecommunications Politecnico di Torino
Torino, Italy
francesca.vipiana@polito.it

***Abstract*—This work proposes a broadband hybrid dielectric characterization method of lossy solid highly variable materials such as those employed in manufacturing realistic head phantoms for microwave imaging systems pre-clinical testing. The technique then recovers the permittivity and conductivity in the range of microwaves, posing the characterization as multi-objective optimization that exploits numerical and measured data. It copes with the intrinsic limitations of traditional dielectric characterization approaches while compensating for measuring errors, combining coaxial probe and double-ridged waveguide scattering measurements in a single scheme. Finally, the characterization is experimentally tested with mimicked head tissues made of custom-made graphite powder and polyurethane mixtures, retrieving their complex permittivity in the band from 1−4 GHz.**

***Index Terms*—Dielectric characterization, double-ridged waveguide, coaxial probe, head model, microwave propagation, optimization.**

I. Introduction

The pre-clinical testing of medical devices is essential to its multiple-stage assessment process, which in the early stages proves the technology concept and, in the last ones, arrives at more sophisticated and realistic validations using mimicked clinical situations. In this context, the phantoms are paramount to development and validation. For instance, authors in [1]–[4] present different typologies of head and breast phantoms used to test medical microwave-based devices to diagnose and follow up brain stroke and cancer detection, respectively.

We can classify the phantoms emulating the dielectric properties of biological tissues in the microwave range, such as the head, into two families based on the type and state of material used for their realization: (1) liquid-based and (2) semi-solid and solid. Then, for the former, the phantoms consist of containers filled with liquid blends combining water with Triton X-100 or alcohol, of which percentages allow it to obtain the target permittivity in the tested device's operation frequency [5]–[7]. However, they have the drawback that might include plastic shells, which add a non-realistic clinical feature to the testing and limit the modeling of multi-tissue ones. For the latter, semi-solid materials like agar-based ones, e.g., gelatine, present a suitable alternative to building complex models [8]–[11]. Nevertheless, they have the challenge of long-term preservation, restricting their use to single-time experiments. With that in mind, different authors have opted to use solid materials such as mixtures of urethane rubber and graphite powder, carbon-loaded plastic, or a combination of these to build complex multi-tissue phantom [12]–[14]. These contribute to structural strength while remaining physically and electrically stable over time. Yet, these materials present a significant challenge when being characterized [15]–[20].

Traditional and well-known techniques, such as the open coaxial probe or resonance-based methods, are unsuitable for a broadband characterization of solid materials. For instance, the open coaxial probe, which fits to characterize liquid mixtures, uses the reflection coefficient measured through a probe immersed in a material sample under test (MUT) and lumped circuit models to retrieve the dielectric properties (DP) [19], [21], [22]. This approach exploits a standard calibration procedure measuring the probe reflection coefficient of three known standards, open, short, and load (such as distilled water), to obtain the calibration coefficient applied later to the MUT measure, retrieving its corresponding DP [23]–[25]. However, the technique only applies to materials with even and smooth surfaces due to the need to ensure controlled pressure and perfect contact between the probe's surface and the MUT. Hence, resonance-based techniques are preferable for solid materials [26]–[28]. These compensate for punctual measuring errors and sample inhomogeneities, as their resonances, and thus, the scattering response, rely

on a more extensive domain. However, these might require detailed mathematical modeling of the resonance device (planar resonant microstrip, waveguide), not always trivial, to extract the permittivity—besides, limitations on bandwidth [15], [17], [18].

Considering the limitation of traditional methods for the characterization of solid materials, we propose a hybrid method employing both numeric and measured data to perform broadband dielectric characterization of mimicked human tissues used to design realistic phantoms, though not limited to these. This technique involves two approaches, the coaxial probe and the waveguide ones, through a multi-objective optimization, derivating dielectric properties of dispersive and lossy materials. Hence, it overcomes the fundamental limitations at the same time, empowers their best features.

In the following, Sect. II mathematically states the method. Sect. III presents its experimental validation, applying it to the characterization of rubber-graphite-based materials mimicking human head tissues in the band from $1-4$ GHz and using a coaxial probe and double-ridged waveguide setups. Finally, Sect. IV describes and analyses the results, while the conclusion and perspectives are discussed in Sect. V.

II. Mathematical Statement Hybrid Method

We propose approaching the broadband characterization of a material as an optimization problem, where the objective is to retrieve the DP of a sample of a lossy solid MUT via the minimization of the differences between the numerical and measured 2-ports scattering response, with a clever initial condition. So, we state a multi-objective cost function that joins the effect of a dispersed complex permittivity, i.e., not constant in frequency and including losses, in a single merit figure that comprehends reflection and transmission effects, as seen in 1, extending the degrees of freedom, the search domain, and its applicability. Moreover, a weighing variable, k, linearly balances the information the permittivity and conductivity provide on the scattering response, thus in the DP retrieving. For instance, in the case of a very lossy material, where the imaginary part of the permittivity might have had a significant influence on the S-parameters, the optimization will tend to weigh more this effect on the cost function.

$$\text{cost} = \Lambda_{\text{diff}}(\mathcal{S}_{11}) \cdot k + \Lambda_{\text{diff}}(\mathcal{S}_{12}) \cdot (1-k), k \in [0,1] \quad (1)$$

On the other hand, the cost individually considers the effects of the reflection and transmission, merging each via an evenly average sum of the square difference over the whole frequency band, as shown by 2, where N represents the number of frequency points. In 2, $\mathcal{S}^{\text{goal}}$ is either the measured $\mathcal{S}_{11}$ or $\mathcal{S}_{12}$ from the resonance device in the studied band, equivalent to $\mathcal{S}_{22}$ and $\mathcal{S}_{21}$ because we consider a symmetrical architecture and anisotropic materials. Meanwhile, $\mathcal{S}^{\text{fitness}}$, the indirect optimization variable, results from a full-wave simulation that models the resonant device and the sample of the MUT, modeled as a homogeneous material whose dielectric properties act as direct optimization variables, $\boldsymbol{\varepsilon}$ (permittivity), $\boldsymbol{\sigma}$ (conductivity). Specifically, to reduce the optimization's complexity, we select three points in the band for both real and imaginary parts as optimization variables, i.e., $[\varepsilon_{f_n}, \sigma_{f_n}]$, where f_n stands by frequency point and $n = [1:3]$. This assumption considers the smooth frequency variation of the complex permittivity of the studied mimicked human head tissues. However, the simulations run a third-degree polynomial interpolation of those, which is then used to produce a response in the same frequency points of the goal as $\text{OP}(\hat{\boldsymbol{\varepsilon}}, \hat{\boldsymbol{\sigma}}) = \mathcal{S}^{\text{fitness}}_{1\times N}$, where OP represents the EM solver, and $\hat{\boldsymbol{\varepsilon}}$ and $\hat{\boldsymbol{\sigma}}$ are the interpolated ones. Such difference also take into account the phase of the scattering parameters. This approach introduces additional constraints in the optimization problem. However, it requires good consistency between reference planes in simulation and measurement.

$$\Lambda_{\text{diff}} = \sqrt{\frac{1}{\text{N}} \sum^{\text{N}} \left| \mathcal{S}^{\text{goal}} - \mathcal{S}^{\text{fitness}} \right|^2} \quad (2)$$

Moving to the optimizer selection, we opt for a trust region optimizer, which searches for the local minimum of the cost function within a trust region in the vicinity of an initial guess [29]. Hence, this produces a fast convergence with a good estimation as long as the initial guess is well-defined. Hence, we consider the DP retrieved using the open-coaxial probe approach to determine the initial guess described in the introduction.

III. Validation

A. Phantom manufacturing

To validate the characterization method, we prepared MUT samples using mixtures with different percentages of urethane rubber and graphite powder molded as $20 \times 18 \times 12$ mm bricks, mimicking the DP of head tissues in the frequency band between $1-4$ GHz, which is of interest for different microwave-based sensing and imaging applications [1], [30], [31]. Thus, the sample dimensions allows the minimum field distribution required to obtain a good estimation of initial condition of the optimizer, being around a height of 10 mm for the used coaxial prove, as well as, fits holding gap in the waveguide [26].

Moreover, we follow a three-step procedure to obtain samples as homogenous as possible. First, we blended the rubber, still liquid, and powder, inserting it gradually into the mixture, using an electronic mixer while applying different speed profiles as depicted in Fig. 1a. Second, the mixture is deposited in 3D molds and moved into a vacuum chamber for around 20 minutes (see Fig. 1b). This step removes the air bubbles in the sample that may cause changes in the DP of the MUTs. Finally, the MUTs is cured for about 12 hours, after which the DP are measured. Figure 1c shows a brain made with a mixture of urethane rubber and graphite powder [14].

B. Experimental Setup and Procedures

1) Coaxial Probe: Figure 2 shows the set up of measurements highlighting the vector network analyzer (VNA) Keysight N5227A and the dielectric probe Agilent 85070D. We use the Keysight "N1500a materials measurement suite" software to take the measurements [32]. The experiment is carried out at room temperature. First, three simultaneous measurements are made for calibration where water is used

(a) (b)

(c)

Fig. 1: Samples preparation: (a) mixer; (b) vacuum chamber; (c) brain made with a mixture of urethane rubber and graphite.

as the known material. Then the sample is measured. In order to have the most reliable measurements possible, the face of the sample with the least imperfections is chosen and constant pressure is maintained with the probe throughout the measurement.

2) Waveguide: To obtain our $\mathcal{S}^{\text{goal}}$, we use a custom ridge waveguide exited via two coaxial-fed rectangular waveguide sections. It consists of a metallic hollow structure that confines the electromagnetic waves in a controlled manner with minimal energy loss, and the geometrical parameters of the cross-section, particularly the ridges, determine its impedance and cut-off frequency. Here, the cut-off frequency is about 1 GHz, so the dominant mode propagates above this, defining the lower operating frequency. Then, after performing a reflection line calibration procedure, the MUT is placed between the ridges that hold it, as shown in Fig. 3, and a VNA HP-8510C measures the scattering parameters. The Thru-Reflection-Line (TRL) Calibration is performed using the empty sample holder in Fig. 3b as line standard, the direct connection of waveguides in Fig. 3a as thru and a full metal block (not shown) as short. Similarly to [33], the TRL calibration defines the reference planes at the ridge waveguide ports i.e. at the sample holder ports. In this way, the effects of waveguide launchers, cables and VNA electronics are properly removed from the measured data. This approach allows for a consistent comparison between measured and simulated data.

From a numerical point of view, we employ CST microwave studio for the full-wave simulations, modeling the system as the section of the ridge waveguide with perfect electric conductor (PEC) walls and fed by two waveguide ports. Moreover, to speed up the execution of the simulations, these are set with twenty-one frequency points. Thus, the optimization considers the same sub-set of points from the measures.

IV. Results

This section exemplifies the characterization procedure with two different mixtures: (1) represents the white matter, and (2) a matching medium that is used in the manufacture of antennas to improve field penetration into head tissue [1]. Figure 4 shows the reflection and transmission measured scattering parameters with the waveguide (solid line) used as the optimization goal. Also, it presents the initial condition (dash-dot line), which was obtained from a simulation using the complex permittivity computed via the open-coaxial method as input parameter. Then, the dashed line depicts the optimized response. These results show how the optimization is able to match the goal after it reaches the convergence, as displayed by the cost function trends and the retrieved DP (see Figs. 5, 6). Here, it is worth noticing that the values of the white matter are not precisely the nominal ones reported in [34], which is a limitation of the manufacturing procedure instead of a problem of the characterization.

V. Conclusion and Perspectives

This work proposes an innovative hybrid method to derive the dielectric properties of solid materials in broadband by overcoming the problems encountered with the coaxial probe

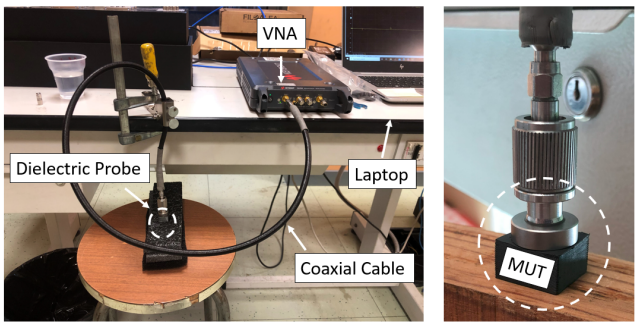

(a) (b)

Fig. 2: Measurements set up: VNA, laptop, coaxial probe and dielectric probe (a) and zoom of a sample (b).

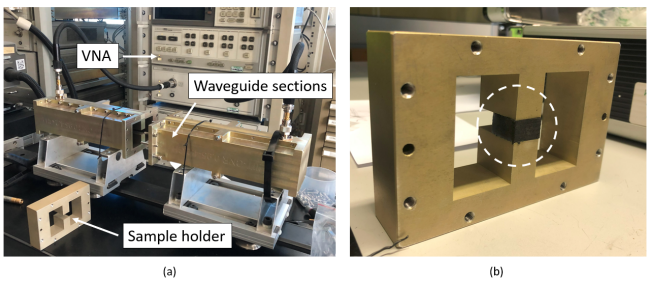

(a) (b)

Fig. 3: System set up (a); sample inserted in the waveguide sample holder (b).

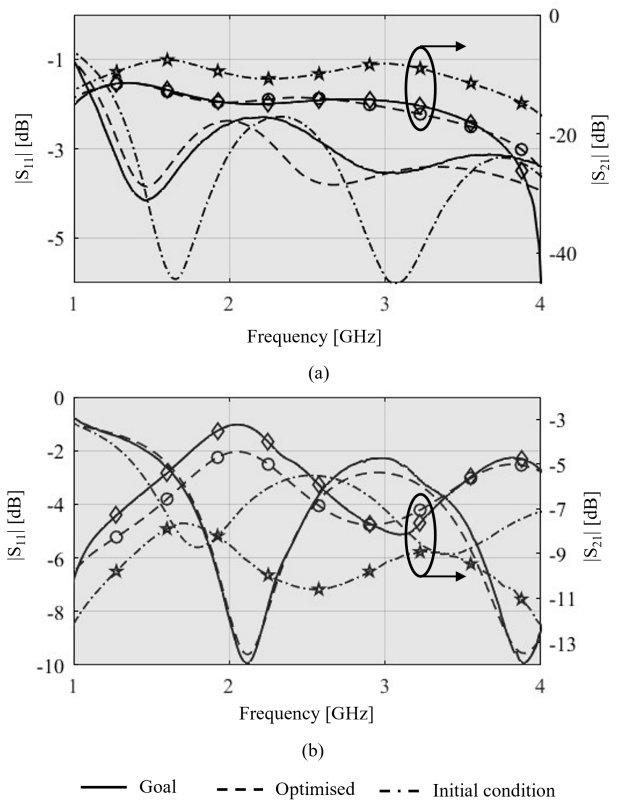

Fig. 4: Reflection and transmission scattering parameters, right and left, respectively. (a) Mimicked white matter, G38. (b) Matching medium, G25.

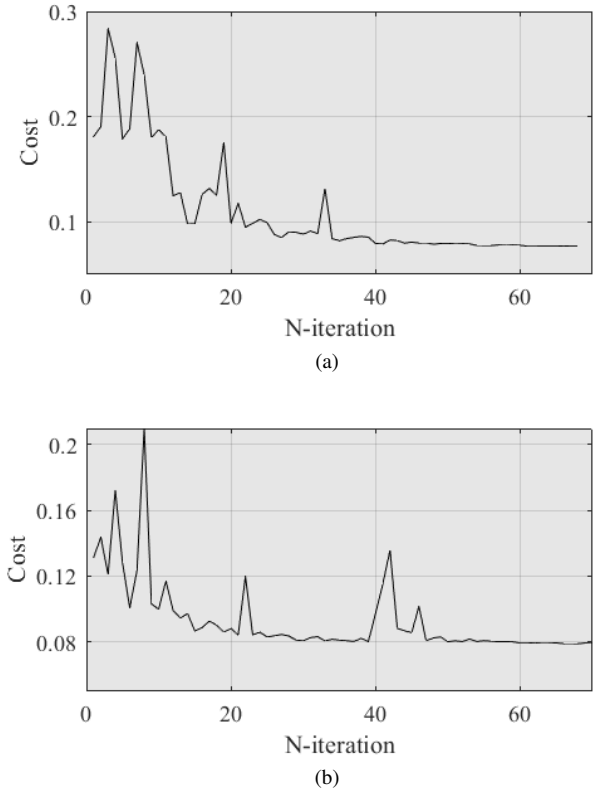

Fig. 5: Trend of the cost function versus the number of iterations of the optimiser of the G25 sample (25% graphite powder and 75% urethane rubber) (a) and the white matter (38% graphite powder and 62% urethane rubber) (b).

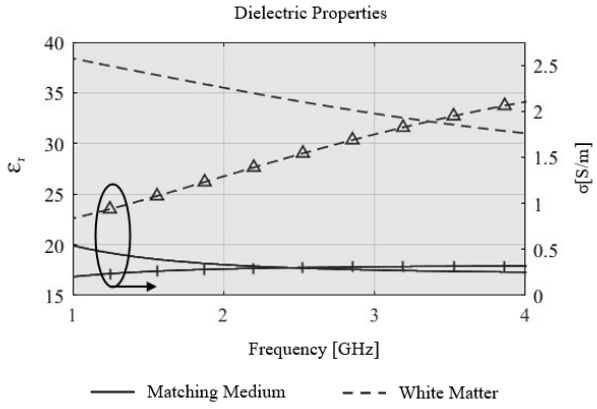

Fig. 6: Permittivity and conductivity of the white matter and the matching medium.

and waveguide. In this specific case, it is applied in the biomedical field, but it can also be extrapolated to other applications, for example, the industrial one. For future work, it is planned to extend the validation in more scenarios and more materials as carbon-loaded plastic.

ACKNOWLEDGMENT

This work was supported in part by the project PON Research and Innovation "Microwave Imaging and Detection powered by Artificial Intelligence for Medical and Industrial Applications (DM 1062/21)", funded by MUR, in part by the project "INSIGHT – An innovative microwave sensing system for the evaluation and monitoring of food quality and safety", funded by MAECI and in part by the project "THERAD - Microwave Theranostics for Alzheimer's Disease", funded by Compagnia di San Paolo. It was carried out partially within the Agritech National Research Center, funded by the European Union Next-Generation EU (Piano Nazionale di Ripresa e Resilienza (PNRR) – MISSIONE 4 COMPONENTE 2, INVESTIMENTO 1.4 – D.D. 1032 17/06/2022, CN00000022).
We thank Prof. Elisa Fiume, Department of Applied Science and Technology (DISAT) – Polytechnic of Turin, for supporting manufacturing of the samples.

REFERENCES

[1] D. O. Rodriguez-Duarte, C. Origlia, J. A. T. Vasquez, R. Scapaticci, L. Crocco, and F. Vipiana, "Experimental assessment of real-time brain stroke monitoring via a microwave imaging scanner," *IEEE Open Journal of Antennas and Propagation*, vol. 3, pp. 824–835, 2022.

[2] B. McDermott, E. Porter, A. Santorelli, B. Divilly, L. Morris, M. Jones, B. Mc Ginley, and M. O'Halloran, "Anatomically and dielectrically realistic microwave head phantom with circulation and reconfigurable lesions," *Progress In Electromagnetics Research B*, vol. 78, pp. 47–60, 01 2017.

[3] M. R. Casu, M. Vacca, J. A. Tobon, A. Pulimeno, I. Sarwar, R. Solimene, and F. Vipiana, "A cots-based microwave imaging system for breast-cancer detection," *IEEE Transactions on Biomedical Circuits and Systems*, vol. 11, no. 4, pp. 804–814, 2017.

[4] A. Fasoula, L. Duchesne, J. D. Gil Cano, P. Lawrence, G. Robin, and J.-G. Bernard, "On-site validation of a microwave breast imaging system, before first patient study," *Diagnostics*, vol. 8, no. 3, 2018. [Online]. Available: https://www.mdpi.com/2075-4418/8/3/53

[5] N. Joachimowicz, B. Duchêne, C. Conessa, and O. Meyer,

"Anthropomorphic breast and head phantoms for microwave imaging," *Diagnostics*, vol. 8, no. 4, 2018. [Online]. Available: https://www.mdpi.com/2075-4418/8/4/85

[6] T. Henriksson, N. Joachimowicz, C. Conessa, and J.-C. Bolomey, "Quantitative microwave imaging for breast cancer detection using a planar 2.45 ghz system," *IEEE Transactions on Instrumentation and Measurement*, vol. 59, no. 10, pp. 2691–2699, 2010.

[7] M. Romeo, L. Di Donato, O. Bucci, I. Catapano, L. Crocco, M. Scarfì, and R. Massa, "Dielectric characterization study of liquid-based materials for mimicking breast tissues," *Microw. Opt. Technol. Lett.*, vol. 53, no. 6, pp. 1276–1280, 2011.

[8] M. Lazebnik, E. L. Madsen, G. R. Frank, and S. C. Hagness, "Tissue-mimicking phantom materials for narrowband and ultrawideband microwave applications," *Physics in Medicine & Biology*, vol. 50, pp. 4245 – 4258, 2005.

[9] E. Porter, J. Fakhoury, R. Oprisor, M. Coates, and M. Popović, "Improved tissue phantoms for experimental validation of microwave breast cancer detection," in *Proceedings of the Fourth European Conference on Antennas and Propagation*, 2010, pp. 1–5.

[10] M. Ostadrahimi, R. Reopelle, S. Noghanian, S. Pistorius, A. Vahedi, and F. Safari, "A heterogeneous breast phantom for microwave breast imaging," in *2009 Annual International Conference of the IEEE Engineering in Medicine and Biology Society*, 2009, pp. 2727–2730.

[11] M. Klemm, J. A. Leendertz, D. Gibbins, I. J. Craddock, A. Preece, and R. Benjamin, "Microwave radar-based breast cancer detection: Imaging in inhomogeneous breast phantoms," *IEEE Antennas and Wireless Propagation Letters*, vol. 8, pp. 1349–1352, 2009.

[12] A. Fasoula, J.-G. Bernard, G. Robin, and L. Duchesne, "Elaborated breast phantoms and experimental benchmarking of a microwave breast imaging system before first clinical study," in *12th European Conference on Antennas and Propagation (EuCAP 2018)*, 2018, pp. 1–5.

[13] B. Mohammed, K. Bialkowski, S. Hill, A. Stancombe, A. Alqadami, M. T. Heitzmann, and A. Abbosh, "Stable and lifelong head phantoms using polymer composition mimicking materials to test electromagnetic medical imaging systems," *IEEE Journal of Electromagnetics, RF and Microwaves in Medicine and Biology*, vol. 5, no. 4, pp. 322–328, 2021.

[14] C. Origlia, M. Gugliermino, D. O. Rodriguez-Duarte, J. A. Tobon Vasquez, and F. Vipiana, "Anthropomorphic multi-tissue head phantom for microwave imaging devices testing," in *2023 17th European Conference on Antennas and Propagation (EuCAP)*, 2023, pp. 1–4.

[15] J. Hu, A. Sligar, C.-H. Chang, S.-L. Lu, and R. Settaluri, "A grounded coplanar waveguide technique for microwave measurement of complex permittivity and permeability," *IEEE Transactions on Magnetics*, vol. 42, no. 7, pp. 1929–1931, 2006.

[16] A. La Gioia, E. Porter, I. Merunka, A. Shahzad, S. Salahuddin, M. Jones, and M. O'Halloran, "Open-ended coaxial probe technique for dielectric measurement of biological tissues: Challenges and common practices," *Diagnostics*, vol. 8, no. 2, 2018.

[17] L. Wang, R. Zhou, and H. Xin, "Microwave (8–50 ghz) characterization of multiwalled carbon nanotube papers using rectangular waveguides," *IEEE Transactions on Microwave Theory and Techniques*, vol. 56, no. 2, pp. 499–506, 2008.

[18] M. Hossain, N. Nguyen-Trong, A. S. Alqadami, and A. M. Abbosh, "Calibrated broadband measurement technique for complex permittivity and permeability," *IEEE Transactions on Microwave Theory and Techniques*, vol. 68, no. 8, pp. 3580–3591, 2020.

[19] A. Tieri, S. Pisa, E. Piuzzi, F. Frezza, and M. Cavagnaro, "Wideband measurement of dielectric properties of wheat flour," *IEEE Transactions on Instrumentation and Measurement*, vol. 72, pp. 1–9, 2023.

[20] M. Berezhanska, D. M. Godinho, P. Maló, and R. C. Conceição, "Dielectric characterization of healthy human teeth from 0.5 to 18 ghz with an open-ended coaxial probe," *Sensors*, vol. 23, no. 3, 2023.

[21] M. Savazzi, D. M. Godinho, N. Ištuk, T. Castela, M. L. Orvalho, E. Porter, M. O'Halloran, C. A. Fernandes, J. M. Felício, and R. C. Conceição, *The Dielectric Properties of Axillary Lymph Nodes*. Cham: Springer International Publishing, 2023, pp. 235–272. [Online]. Available: https://doi.org/10.1007/978-3-031-28666-7_8

[22] A. La Gioia, E. Porter, I. Merunka, A. Shahzad, S. Salahuddin, M. Jones, and M. O'Halloran, "Open-ended coaxial probe technique for dielectric measurement of biological tissues: Challenges and common practices," *Diagnostics*, vol. 8, no. 2, p. 40, 2018.

[23] A. Kraszewski, M. A. Stuchly, and S. S. Stuchly, "Ana calibration method for measurements of dielectric properties," *IEEE Transactions on Instrumentation and Measurement*, vol. 32, no. 2, pp. 385–387, 1983.

[24] M. A. Stuchly and S. S. Stuchly, "Coaxial line reflection methods for measuring dielectric properties of biological substances at radio and microwave frequencies-a review," *IEEE Transactions on Instrumentation and Measurement*, vol. 29, no. 3, pp. 176–183, 1980.

[25] M. Cavagnaro and G. Ruvio, "Numerical sensitivity analysis for dielectric characterization of biological samples by open-ended probe technique," *Sensors*, vol. 20, no. 13, p. 3756, 2020.

[26] G. Addamo, G. Virone, D. Vaccaneo, R. Tascone, O. A. Peverini, and R. Orta, "An adaptive cavity setup for accurate measurements of complex dielectric permittivity," *Progress In Electromagnetics Research*, vol. 105, pp. 141–155, 2010.

[27] M. I. Hossain, N. Nguyen-Trong, A. S. M. Alqadami, and A. M. Abbosh, "Calibrated broadband measurement technique for complex permittivity and permeability," *IEEE Transactions on Microwave Theory and Techniques*, vol. 68, no. 8, pp. 3580–3591, 2020.

[28] T. Alam and M. Cheffena, "Integrated microwave antenna/sensor for sensing and communication applications," *IEEE Transactions on Microwave Theory and Techniques*, vol. 70, no. 11, pp. 5289–5300, 2022.

[29] M. H. Bakr, J. W. Bandler, R. M. Biernacki, S. H. Chen, and K. Madsen, "A trust region aggressive space mapping algorithm for em optimization," *IEEE Transactions on Microwave Theory and Techniques*, vol. 46, no. 12, pp. 2412–2425, 1998.

[30] T. Pokorny, D. Vrba, J. Tesarik, D. B. Rodrigues, J. Vrba *et al.*, "Anatomically and dielectrically realistic 2.5 d 5-layer reconfigurable head phantom for testing microwave stroke detection and classification," *International Journal of Antennas and Propagation*, vol. 2019, 2019.

[31] A. Mobashsher and A. Abbosh, "Three-dimensional human head phantom with realistic electrical properties and anatomy," *IEEE Antennas and Wireless Propagation Letters*, vol. 13, pp. 1401–1404, 2014.

[32] "An1500a materials measurement suite," Available at https://www.keysight.com/it/en/product/N1500A/materials-measurement-suite.html.

[33] L. Valenziano, O. Peverini, M. Zannoni, R. Tascone, G. Addamo, G. Virone, M. Lumia, S. Mariotti, and A. De Rosa, "New rf data on eccosorb cr/mf absorber," in *Millimeter, Submillimeter, and Far-Infrared Detectors and Instrumentation for Astronomy VII*, vol. 9153. SPIE, 2014, pp. 937–943.

[34] "An internet resource for the calculation of the dielectric properties of body tissues in the frequency range 10 Hz - 100 GHz," Available at http://niremf.ifac.cnr.it/tissprop/htmlclie/htmlclie.php.